Available online at www.sciencedirect.com
SCIENCE DIRECT
Polymer 46 (2005) 2354–2364
polymer
www.elsevier.com/locate/polymer

Thermal properties, specific interactions, and surface energies of PMMA terpolymers having high glass transition temperatures and low moisture absorptions

Jem-Kun Chen, Shiao-Wei Kuo, Hsin-Ching Kao, Feng-Chih Chang*

Institute of Applied Chemistry, National Chiao Tung University, Hsin Chu, Taiwan, ROC

Received 18 June 2004; received in revised form 15 November 2004; accepted 27 January 2005

Abstract

We have prepared a series of poly(methyl methacrylate) (PMMA)-based terpolymers that have high glass transition temperatures and low moisture absorptions by the free radical copolymerization of methyl methacrylate, methacrylamide, and styrene in dioxane. We have investigated the effects of the styrene content on the glass transition temperatures, hydrogen bonding interactions, surface energies, moisture absorption, and molecular weights of these poly(methyl methacrylate-*co*-methacrylamide-*co*-styrene) (Poly(MMA-*co*-MAAM-*co*-S)) terpolymers by differential scanning calorimetry, Fourier transform infrared and X-ray photoelectron spectroscopies, contact angle measurements, and gel permeation chromatography. The results indicate that the glass transition temperatures, hydrogen bonding strengths, surface energies, molecular weights, and the moisture absorption decreased upon increasing the PS content in most of the terpolymer systems. In addition, the moisture absorptions of some selected terpolymers decreased even through they possess higher values of T_g than pure PMMA. These selected terpolymers have the potential to replace pure PMMA in optical device applications.

Keywords: Hydrogen bonding; Surface energy; Moisture absorption

1. Introduction

Polymers possessing high glass transition temperatures are attractive materials in the polymer industry. For instance, the poly(methyl methacrylate) (PMMA) is a transparent polymeric material possessing many excellent properties, such as light weight, high light transmittance, chemical resistance, colorlessness, weathering corrosion resistance, and good insulation [1]. The glass transition temperature of PMMA, however, is relatively low at ca. 100 °C, which limits its applications in optical-electronic industries—such as compact disc (CD), optical glass, and optical fiber production—because it undergoes distortion when used in an inner glazing material [2–3]. Previously, we suggested an approach to raise the value of T_g of PMMA through copolymerization with methacrylamide (MAAM) because strong hydrogen bonding interactions exist between these two monomer segments [4]. It is well known, however, that the moisture absorption of polymers increases when hydrogen bonding interactions exist, which again limits their applications in optical-electronic industries. In this paper, we offer a novel approach to reduce the moisture absorption of such hydrogen-bonded copolymers through their copolymerization with another inert diluent segment—styrene.

In this work, we choose to copolymerize MMA, MAAM, and styrene, rather than simply create a ternary polymer blend of PMMA/PMAAM/PS, for three reasons: (1) simple polymer blending results in phase separation problems because totally miscible ternary blends are rare; (2) the value of T_g of the copolymer is generally higher than that of the corresponding polymer blend because, as it has been reported widely, compositional heterogeneities exist in hydrogen bonded copolymers [5–6]; (3) styrene plays a role strictly as an inert diluent segment on the PMAAM main chain [7]. The latter feature offers an opportunity to

* Corresponding author. Tel.: +886 3 572 7077; fax: +886 3 571 9507.
E-mail address: changfc@mail.nctu.edu.tw (F.-C. Chang).

0032-3861/$ - see front matter © 2005 Elsevier Ltd. All rights reserved.
doi:10.1016/j.polymer.2005.01.046

enhance the specific interactions between the amide groups of PMAAM and the functional groups of the second polymer by reducing the strong self-association of PMAAM units, which we have discussed previously [7].

Generally, hydrogen bonding can be characterized by Fourier transform infrared spectroscopy (FTIR) because such interactions affect local electron densities and, consequently, frequency shifts can be observed [8–10]. Recently, X-ray photoelectron spectroscopy (XPS) has also been used to study the specific interactions between metal ions and ligands in polymer blends [11–13]. The development of a new peak or shoulder usually can be observed in the XPS spectrum when the chemical environment of an atom in a polymer blend or copolymer is perturbed as a result of a specific interaction. In addition, surface enrichment in copolymers has been studied extensively, but surface segregation with respect to specific interactions, such as hydrogen bonding, has received little attention. In this study, we examined the thermal properties of poly (methyl methacrylate-*co*-methacrylamide-*co*-styrene) (poly(MMA-*co*-MAAM-*co*-S)) terpolymers by using differential scanning calorimetry (DSC). We have investigated (1) the effects that hydrogen bonding interactions exert on these systems by using Fourier transform infrared spectroscopy (FTIR) and X-ray photoelectron spectroscopy (XPS), (2) the molecular weights by using gel permeation chromatography (GPC), and (3) the use of contact angle measurements for calculating surface energies. In addition, we have studied the effects of the hydrogen bonding interactions on the surface segregation of a series of Poly(MMA-*co*-MAAM-*co*-S) terpolymers.

2. Experimental

2.1. Materials

Methyl methacrylate, methacrylamide, and styrene monomers were purchased from the Aldrich Chemical Company; they were purified by distillation under vacuum and a nitrogen atmosphere before polymerization. The radical initiator azobisisobutyronitrile (AIBN) was recrystallized from ethyl alcohol prior to use. 1,4-Dioxane was distilled under vacuum and then used as the solvent for the copolymerization experiments performed in solution.

2.2. Syntheses of poly(methyl methacrylate-co-methacrylamide-co-styrene) terpolymers

The solution copolymerization of methyl methacrylate, styrene, and methacrylamide was carried out in 1,4-dioxane at 80 °C under a nitrogen atmosphere in a glass reaction flask equipped with a condenser. AIBN (1 wt% based on monomers) was employed as the initiator. The mixture was stirred for ca. 24 h before being poured into excess isopropyl alcohol under vigorous agitation to precipitate the product. The crude copolymer product was purified by redissolving it in 1,4-dioxane and then adding this solution dropwise into a large excess of isopropyl alcohol. This procedure was repeated several times and then the residual solvent of the final product was removed under vacuum at 70 °C for 1 day to yield pure white poly(methyl methacrylate-*co*-methacrylamide-*co*-styrene). The chemical composition of the copolymer was determined by the use of elemental analysis and ^{1}H NMR spectroscopy [4,7].

2.3. Characterization

Molecular weights and molecular weight distributions were determined by gel permeation chromatography (GPC) using a Waters 510 HPLC system—equipped with a 410 Differential Refractometer, a UV detector, and three Ultrastyragel columns (100, 500, and 10^3 Å) connected in series in order of increasing pore size—using THF as an eluent at a flow rate of 0.4 mL/min. A molecular weight calibration curve was obtained using polystyrene standards. The elementary analyses (EA) of N, C, and H atoms in the polymers were determined using auto-elementary analysis equipment and applying helium as the carrier gas. The glass transition temperature of the copolymer was determined using a Du-Pont DSC-9000 DSC system. The samples were kept at 280 °C for 3 min and then they were cooled quickly to 30 °C from the melt of the first scan. The value of T_g was obtained as the inflection point of the jump heat capacity at a scan rate of 20 °C/min within the temperature range 30–280 °C. All measurements were conducted under a nitrogen atmosphere. Infrared spectra of the copolymer films were determined by using the conventional NaCl disk method. The 1,4-dioxane solution containing the blend was cast onto a NaCl disk. The film used in this study was thin enough to obey the Beer–Lambert law. FTIR measurements were performed on a Nicolet Avatar 320 FTIR spectrophotometer; 32 scans were collected at a spectral resolution of 1 cm^{-1}. ^{1}H NMR spectra of these copolymers were recorded on a Brucker ARX300 spectrometer using $CDCl_3$ as the solvent. XPS measurements were undertaken on a VG Scientific MicroLab310F UK spectrometer equipped with an Al Kα standard and a hemispherical energy analyzer. The X-ray source was operated at 12 kV and 10 mA; a pass energy of 50 eV was used in the analyzer. The pressure in the analysis chamber was maintained at 10^{-8} mbar or lower during the measurements. All core-level spectra were referenced to the saturated hydrocarbon C 1 s peak at 285.0 eV.

2.4. Surface energy calculations

Contact angles were measured using a Kruss-G40 contact angle goniometer employing the sessile drop principle. The contact angles on both sides of the drop image were measured using at least three liquid drops. The values reported are the means of these measurements

Table 1
Surface tension parameters (in mJ/m^2) of testing liquids

Parameter	Water	Glycerol	Diiodomethane
γ^+	25.5	3.92	0.0
γ^-	25.5	57.4	0.0
γ^{AB}	51.0	30.0	0.0
γ^{LW}	21.8	34.0	50.8
γ	72.8	64.0	50.8

(within $\pm 3°$). The contact angles were measured at 22 ± 2 °C.

Surface energies were evaluated using the Lifshitz–van der Waals acid–base approach (three-liquid acid–base method) that was proposed by van Oss et al. in 1987 [14,15]. This methodology introduces new meanings for the concept of 'apolar' (Lifshitz–van der Waals, γ^{LW}) and 'polar' (Lewis acid–base, γ^{AB}); the latter cannot be represented by a single parameter such as γ^p. Briefly, the theoretical approach follows the additive concept suggested by Fowkes [16]:

$$\gamma = \gamma^d + \gamma^{AB} \tag{1}$$

where γ^d represents the dispersive term of the surface tension. The superscript AB refers to the acid–base interaction. By regrouping the various components in Eq. (1), van Oss et al. expressed the surface energy as

$$\gamma = \gamma^{LW} + \gamma^{AB} \tag{2}$$

In addition, two parameters have been created to describe the strength of the Lewis acid and base interactions: γ^+, the (Lewis) acid parameter of surface free energy, and γ^-, the (Lewis) base parameter of surface free energy.

$$\gamma^{AB} = 2(\gamma_s^+ \gamma_s^-)^{1/2} \tag{3}$$

Van Oss, Good, and their co-workers developed a 'three-liquid procedure' [Eq. (4)] to determine γ_S by the contact angle technique:

$$\gamma_L(1 + \cos\theta) = 2[(\gamma_s^{LW}\gamma_L^{LW})^{1/2} + (\gamma_s^+\gamma_L^-)^{1/2} + (\gamma_s^-\gamma_L^+)^{1/2}] \tag{4}$$

To determine the components of γ_S of a polymer solid, it is recommended that three liquids be selected—two of them polar and the third one apolar. The LW, Lewis acid, and Lewis base parameters of γ_S can then be determined by solving these three equations simultaneously. By measuring contact angles for three well-characterized (in terms of γ_L^{LW}, γ_L^+ and γ_L^-) [17–18] liquids, three equations with three unknowns are generated. We employed water, diiodomethane, and ethylene glycol; their surface energies are provided in Table 1. Each data point is the average of 10 measurements.

3. Results and discussion

3.1. Copolymer analyses

The chemical composition of the methacrylamide (MAAM) monomer was measured by elemental analysis.

Table 2
Poly(MMA-*co*-MAAM-*co*-S) terpolymers synthesized for this study

Polymer	Monomer feed (wt%)			Polymer composition (wt%)			M_w (g/mol.)	T_g (°C)
	PMMA	PMAAM	PS	PMMA	PMAAM	PS		
PMMA	100	0	0	100	0	0	57000	100.0
90-10-0	90	10	0	92.8	7.2	0	54800	126.5
90-8-2[a]	90	8	2	91.0	6.8	2.2	32400	145.3
90-6-4	90	6	4	90.6	5.2	4.2	24800	132.1
90-4-6	90	4	6	90.3	3.5	6.2	20200	125.7
90-2-8	90	2	8	90.0	1.7	8.3	16000	132.3
85-15-0	85	15	0	88.6	11.4	0	38300	144.5
85-12-3	85	12	3	86.4	10.4	3.2	28500	133.2
85-9-6	85	9	6	86.0	7.7	6.3	26800	129.9
85-6-9	85	6	9	85.4	5.2	9.4	25600	125.9
85-3-12	85	3	12	85.0	2.5	12.5	24500	118.1
80-20-0	80	20	0	85.8	14.2	0	22000	149.0
80-16-4	80	16	4	81.8	14.0	4.2	19000	139.1
80-12-8	80	12	8	81.2	10.4	8.4	18000	134.1
80-8-12	80	8	12	80.5	7.0	12.5	12500	132.7
80-4-16	80	4	16	80.0	3.4	16.6	10900	139.2
60-40-0	60	40	0	72.2	28.8	0	35000	203.1
60-32-8	60	32	8	62.8	28.5	8.7	9400	159.6
60-24-16	60	24	16	61.8	21.0	17.2	8800	148.8
60-16-24	60	16	24	60.8	13.8	25.4	7900	146.1
60-8-32	60	8	32	60.0	6.8	33.2	7400	136.7

[a] 90-8-2 is defined by the monomer feed, which means 90 wt% of PMMA, 8 wt% of PMAAM and 2 wt% of PS content in poly(MMA-*co*-MAAM-*co*-S) terpolymers. The other samples are also defined in the same way.

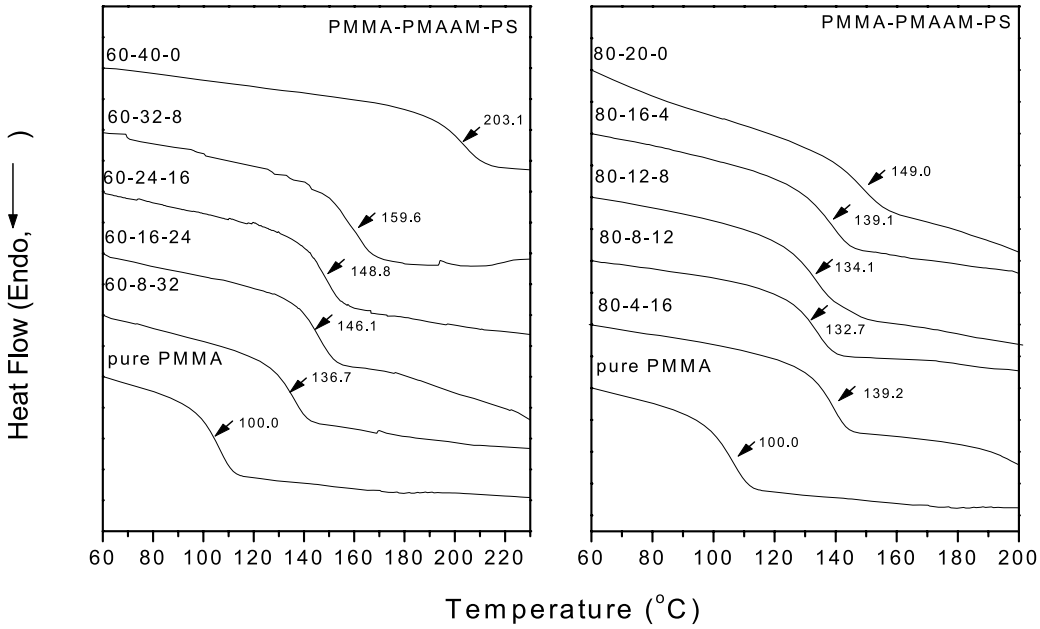

Fig. 1. DSC scans of poly(MMA-*co*-MAAM-*co*-S) copolymers at PMMA contents of 60 and 80 wt%.

In addition, the methyl methacrylate and styrene contents were determined by ^{1}H NMR spectroscopy [4,7]. Table 2 lists all of the monomer feed ratios, copolymer compositions, and molecular weights of the poly(MMA-*co*-MAAM-*co*-S) terpolymers. For convenience, we use the monomer feeds to define the specimen codes since they have the same molecular weight of PMMA content. For example, 90-8-2 means 90 wt% of PMMA, 8 wt% of PMAAM and 2 wt% of PS content in poly(MMA-*co*-MAAM-*co*-S) terpolymers. The reactivity ratios of copolymers have been calculated previously (PMMA-*co*-PMAAM: $r_{PMMA}=1.38$, $r_{PMMAM}=0.24$; PMMA-*co*-PS: $r_{PMMA}=0.5$, $r_{PS}=0.5$; PMAAM-*co*-PS: $r_{PMAAM}=2.04$, $r_{PS}=2.89$) [4,7,19]. Clearly, the reactivity of these monomers in poly(MMA-*co*-MAAM-*co*-S) copolymer systems follows the order PMMA > PS > PMAAM. As a result, the PMMA and PS ratios in these terpolymer systems are greater than their monomer feed ratios, while the PMAAM ratio is lower. Furthermore, the molecular weights of the copolymers decreased upon increasing the contents of PMAAM and PS. This result indicates that the addition of PMAAM or PS causes copolymerization to become difficult because of the polarity difference between PS and PMMA or PMAAM.

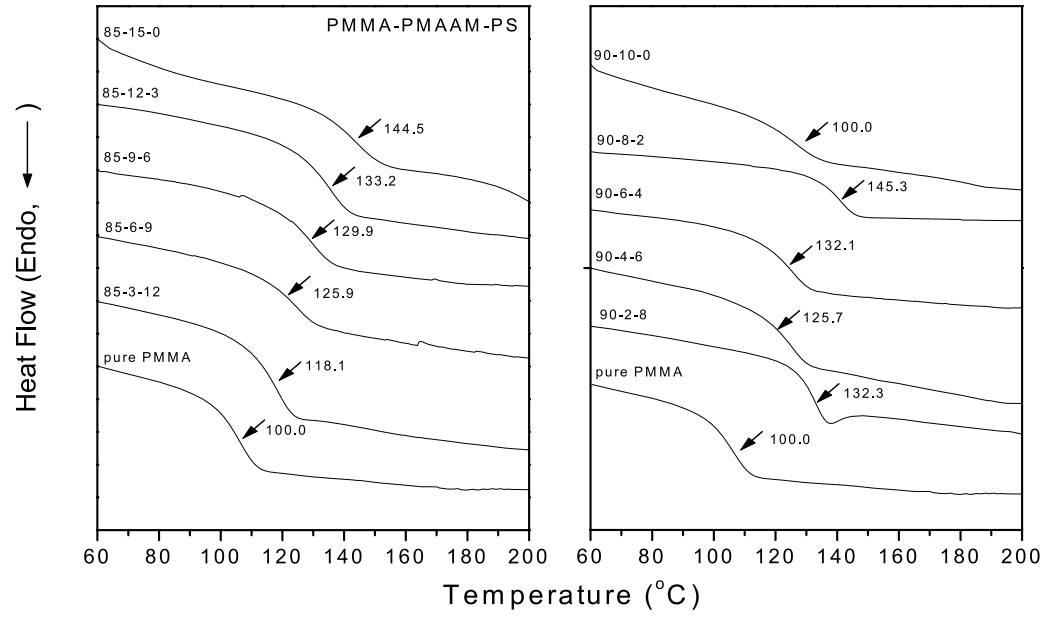

Fig. 2. DSC scans of poly(MMA-*co*-MAAM-*co*-S) copolymers at PMMA contents of 85 and 90 wt%.

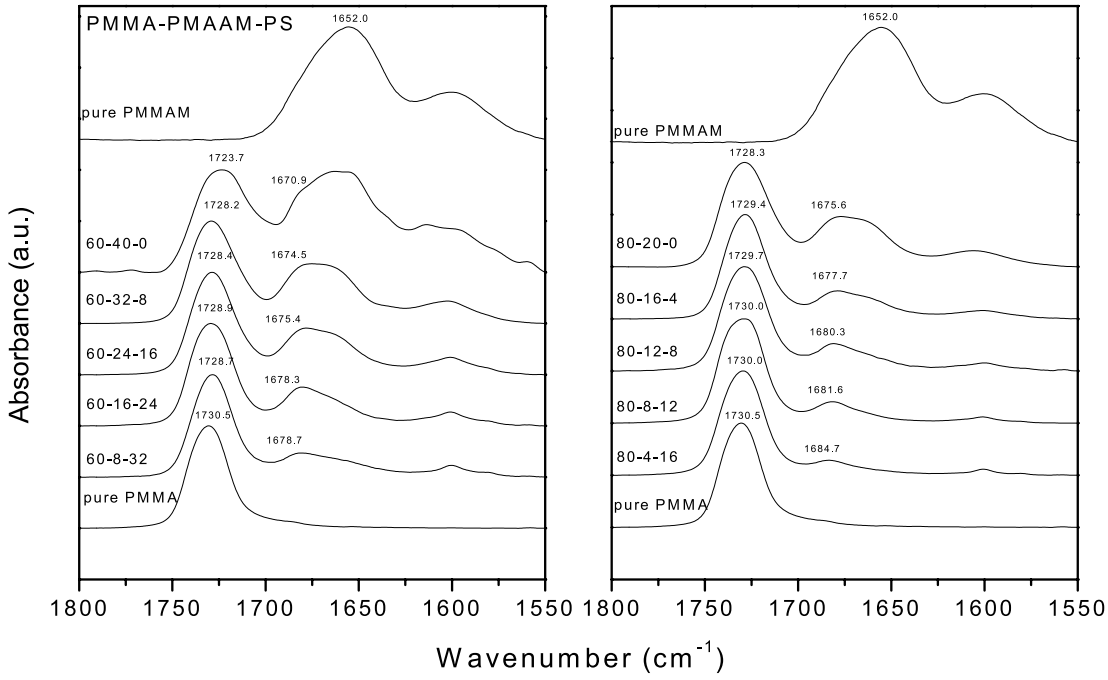

Fig. 3. IR spectra, displaying the range 1550–1800 cm^{-1}, of pure PMMA, pure PMAAM, and poly(MMA-*co*-MAAM-*co*-S) copolymers at PMMA contents of 60 and 80 wt%.

3.2. Thermal and FTIR analyses

Figs. 1 and 2 display the DSC thermograms of pure PMMA and several poly(MMA-*co*-MAAM-*co*-S) terpolymers. All these terpolymers show a single glass transition temperature, indicating that these terpolymers are mostly in short blocks and homogeneous in the range 10–30 nm [4]. Therefore, the incorporation of styrene and methacrylamide monomer into the PMMA main chain can be considered as statistical. When compared with the PMMA-*co*-PMAAM copolymer at same PMMA content, we observe that the value of T_g of the Poly(MMA-*co*-MAAM-*co*-S) terpolymer generally decreases as the PS content increase. This result arises from two factors: (1) the value of T_g of pure PS

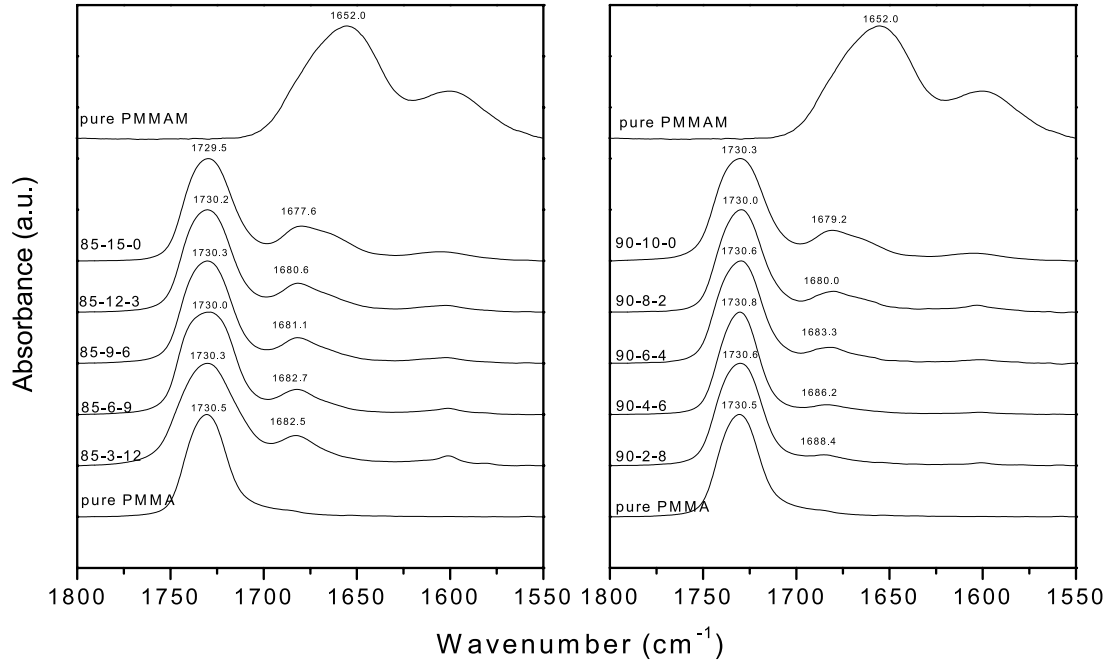

Fig. 4. IR spectra, displaying the range 1550–1800 cm^{-1}, of pure PMMA, pure PMAAM, and poly(MMA-*co*-MAAM-*co*-S) copolymers at PMMA contents of 85 and 90 wt%.

Table 3
Curve fitting of the IR spectra of the copolymers recorded at room temperature

Polymer	Carbonyl in PMMA		Amide I in PMAAM			
	Free C=O		Free Amide I		H-bond Amide I	
	ν (cm^{-1})	A_f (%)	ν (cm^{-1})	A_f (%)	ν (cm^{-1})	A_f (%)
PMMA	1730.5	100.0	–	–	–	–
90-10-0	1730.3	75.7	1679.2	23.0	1657.2	1.3
90-8-2	1730.0	80.9	1680.0	19.0	1657.9	1.1
90-6-4	1730.6	85.1	1683.3	14.6	1658.6	0.3
90-4-6	1730.8	87.4	1686.2	12.5	1653.5	0.1
90-2-8	1730.6	87.9	1688.4	11.5	1652.1	0.6
85-15-0	1729.5	71.9	1677.6	26.9	1656.3	1.2
85-12-3	1730.2	77.8	1680.6	20.7	1656.2	1.5
85-9-6	1730.3	80.7	1681.1	18.0	1656.7	1.3
85-6-9	1730.0	83.6	1682.7	14.0	1661.0	2.4
85-3-12	1730.3	81.3	1682.5	17.8	1654.0	0.9
80-20-0	1728.3	62.7	1675.6	34.4	1656.7	2.9
80-16-4	1729.4	72.5	1677.7	27.0	1657.3	0.5
80-12-8	1729.7	76.9	1680.3	22.0	1653.5	1.1
80-8-12	1730.0	82.7	1681.6	16.1	1656.0	1.2
80-4-16	1730.0	84.7	1684.7	14.6	1651.6	0.7
60-40-0	1723.7	47.2	1670.9	45.3	1650.9	7.5
60-32-8	1728.2	55.9	1674.5	42.2	1657.1	1.9
60-24-16	1728.4	60.5	1675.4	37.5	1654.3	2.0
60-16-24	1728.9	69.2	1678.7	26.8	1655.3	4.0
60-8-32	1728.7	72.1	1678.3	26.5	1649.1	1.4
Pure PMAAM	–	0	1677.0	29.2	1652.0	70.8

(100 °C) is lower than that of PMMA-*co*-PMAAM and (2) the PS monomer plays a role strictly as an inert diluent segment on the PMAAM polymer chain to reduce the strength of its hydrogen bonding. At poly(MMA-*co*-MAAM-*co*-S) compositions of 80/4/16, 90/2/8, and 90/8/2, however, the values of T_g are greater than those of other compositions (at a constant 80 and 90 wt% of PMMA) because PMAAM is able to interact with PMMA effectively through intermolecular hydrogen bonding. In a previous study based on infrared analysis [7], we found that the PS and PMAAM units of the copolymer do not interact specifically, which indicates that the styrene plays a role strictly as an inert diluent segment on the PMAAM main chain. This result offers an opportunity to enhance the specific interactions between the amide groups of PMAAM and the functional groups of a second polymer by reducing the strong self-association of PMAAM. As a result, in some cases, the inter-associative hydrogen bonding increases upon the addition of PS units. In addition, it is worth noting that the glass transition temperatures of all these terpolymers are higher than pure PMMA.

Fourier transform infrared spectroscopy is one of the most powerful tools for identifying and investigating hydrogen bonding in polymers. Figs. 3 and 4 display FTIR spectra, recorded at room temperature, of the PMMA terpolymers. Pure PMAAM exhibits two bands at 1650 and 1600 cm^{-1}, which correspond to the amide I (C=O stretching vibrations) and amide II (N–H bending vibration) bands, respectively. The carbonyl stretching band of pure PMMA located at 1730 cm^{-1} reflects a free carbonyl group. Clearly, the absorption of the amide I group shifts to higher wavenumber as the PMMA content increases and its intensity decreases upon increasing the PMMA content in the PMAAM-*co*-PMMA copolymers, which implies that some of the self-associated hydrogen-bonded amide groups become inter-associated through hydrogen bonding to carbonyl groups of MMA units. When considering the microstructure of the copolymer, the large probability of finding a sequence of only a single MAAM unit suggests that only a small amount of self-associated hydrogen-bonded amide groups of PMAAM units is expected. Therefore, the inter-associated hydrogen bonding is more dominant in the PMAAM-*co*-PMMA copolymer than is the self-associated hydrogen bonding of the pure PMAAM. This absorption also shifts to high wavenumber and its intensity also decreases upon increasing the PS content in the Poly(MMA-*co*-MAAM-*co*-S) copolymers. Furthermore, the carbonyl stretching band of PMMA in the poly(MMA-*co*-MAAM-*co*-S) copolymer shifts to lower wavenumber as the PMAAM content increases. The carbonyl stretching bands located between 1620 and 1800 cm^{-1} are split into three major absorptions, which can be fitted well to the Gaussian function. Table 3 summarizes the results from curve fitting of these spectra and indicates that the carbonyl group band in PMMA shifts to lower wavenumber upon increasing the PMAAM content in the copolymer. In addition, upon increasing the PS content, the free amide I group of PMAAM shifts to higher wavenumber and the fraction of free amide I decreases. This result indicates that hydrogen bonding interactions exist

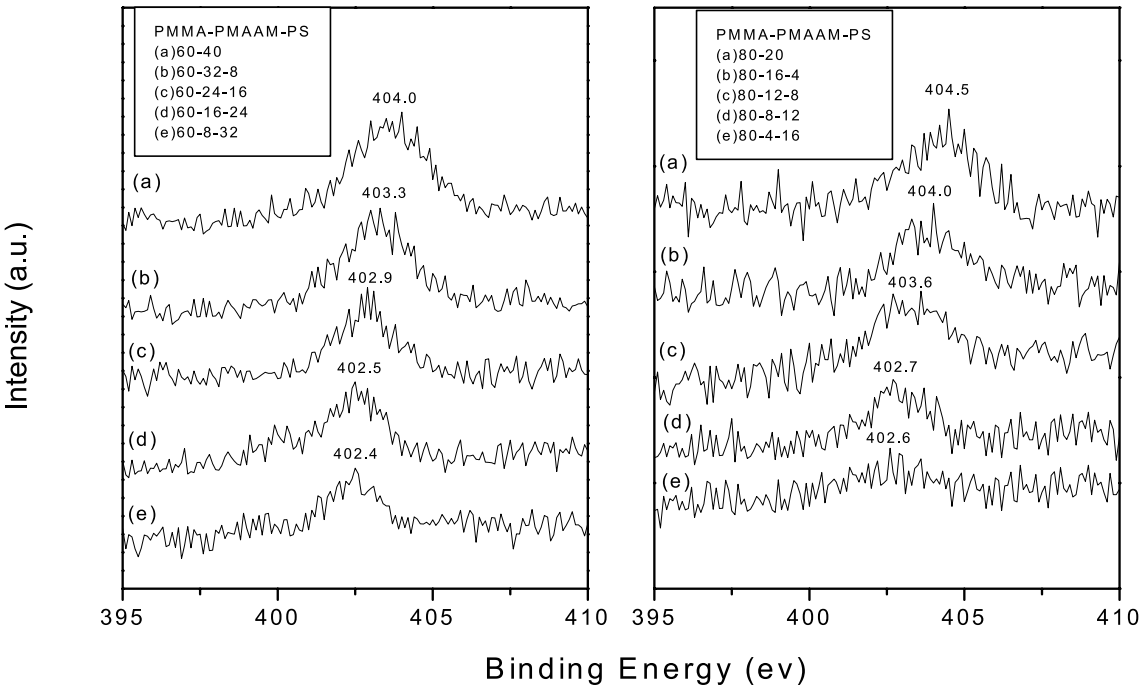

Fig. 5. Nitrogen 1 s core-level X-ray photoelectron spectra of poly(MMA-*co*-MAAM-*co*-S) terpolymers at PMMA contents of 60 and 80 wt%.

between the carbonyl group of PMMA and the amide group of PMAAM and that the styrene units do indeed play the role of inert diluent segments of PMAAM. Furthermore, the area fraction of the amide I band decreases as the PS content increases because the shift of the amide I group to higher wavenumber decreases the absorptivity coefficient. This phenomenon also increases the area fraction of the PMMA content upon increasing the PS content in the copolymers.

3.3. XPS characterization

Fig. 5 displays the N 1 s core-level spectra of poly(MMA-*co*-MAAM-*co*-S) terpolymers at PMMA

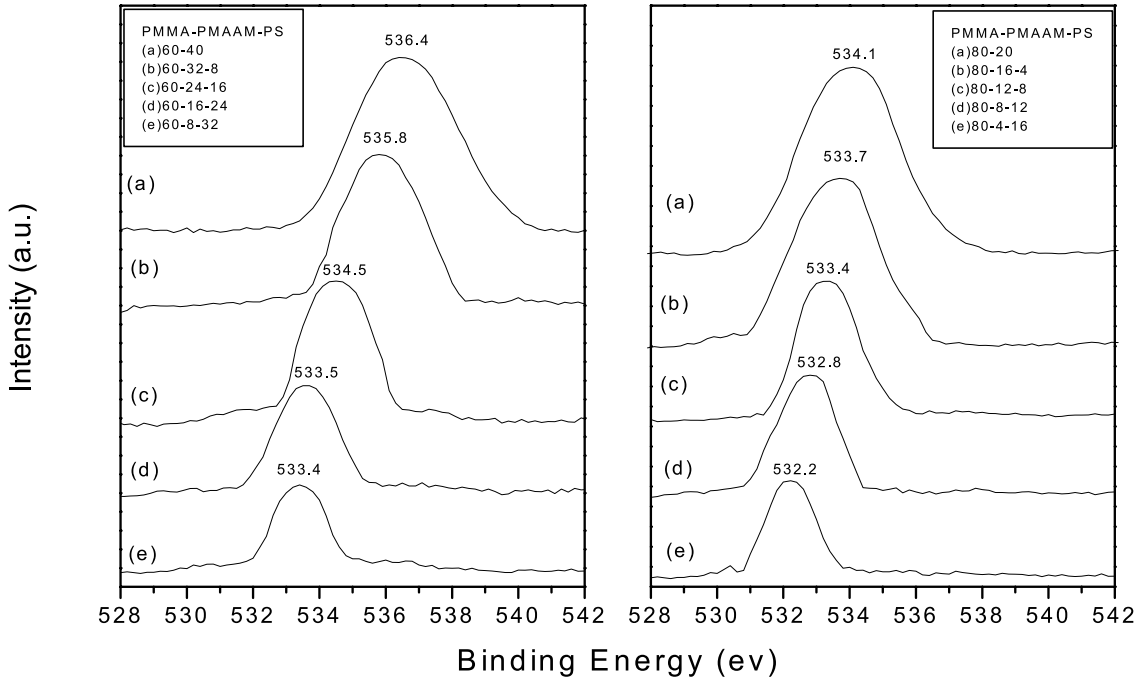

Fig. 6. Oxygen 1 s core-level X-ray photoelectron spectra of poly(MMA-*co*-MAAM-*co*-S) terpolymers at PMMA contents of 60 and 80 wt%.

Table 4
Contact angles of poly(MMA-*co*-MAAM-*co*-S) terpolymers

Compositions PMMA-PMAAM-PS	Contact angles	Water	Glycerol	Diiodo methane
90-10-0	Advancing angle	68.9±1.7	66.6±1.5	39.4±2.1
	Receding angle	55.9±1.6	54.7±2.3	31.5±2.0
90-8-2	Advancing angle	70.3±1.9	67.4±1.8	39.8±1.9
	Receding angle	56.1±2.1	54.3±1.8	32.7±2.4
90-6-4	Advancing angle	70.6±1.3	67.8±2.1	40.7±1.5
	Receding angle	57.2±1.9	54.4±1.3	33.7±1.4
90-4-6	Advancing angle	71.4±2.1	68.3±2.0	41.0±1.8
	Receding angle	57.5±2.0	55.3±1.5	33.9±2.1
90-2-8	Advancing angle	71.4±2.4	68.5±1.4	41.6±1.3
	Receding angle	57.2±1.4	55.1±1.8	33.8±2.2
85-15-0	Advancing angle	66.9±1.1	63.9±2.3	37.0±1.4
	Receding angle	54.1±2.3	51.6±1.9	30.8±1.2
85-12-3	Advancing angle	69.2±1.6	66.4±1.3	39.9±2.0
	Receding angle	56.5±1.5	53.8±1.9	32.1±2.4
85-9-6	Advancing angle	69.0±1.9	66.7±1.8	40.1±1.8
	Receding angle	55.8±2.1	54.2±2.3	32.1±1.4
85-6-9	Advancing angle	71.2±1.6	68.4±2.1	41.8±1.3
	Receding angle	57.5±1.3	55.3±1.6	33.1±1.6
85-3-12	Advancing angle	71.2±1.5	68.5±1.8	42.0±1.4
	Receding angle	57.1±2.1	55.6±1.6	34.8±1.4
80-20-0	Advancing angle	62.9±1.4	60.2±1.3	34.6±1.2
	Receding angle	51.4±1.9	48.6±1.4	28.9±1.1
80-16-4	Advancing angle	64.4±2.0	62.2±1.1	36.2±1.9
	Receding angle	52.9±1.4	50.1±2.3	29.7±1.7
80-12-8	Advancing angle	65.5±1.6	64.5±1.7	41.0±1.8
	Receding angle	53.4±1.8	52.3±1.5	33.8±2.1
80-8-12	Advancing angle	67.9±2.1	66.5±2.2	41.6±2.0
	Receding angle	55.8±2.2	53.1±1.9	33.5±2.2
80-4-16	Advancing angle	69.8±1.3	68.2±1.6	42.9±2.0
	Receding angle	56.4±2.3	55.9±1.5	34.1±1.5
60-40-0	Advancing angle	54.0±1.2	48.5±1.6	27.1±1.6
	Receding angle	43.3±1.7	39.4±1.4	22.7±1.4
60-32-8	Advancing angle	57.3±1.5	52.8±1.4	33.3±1.2
	Receding angle	46.6±1.4	42.2±1.1	27.8±1.1
60-24-16	Advancing angle	60.5±1.8	57.4±1.5	37.9±1.5
	Receding angle	49.4±2.1	46.5±1.6	30.9±1.8
60-16-24	Advancing angle	62.1±1.9	61.5±2.3	42.8±2.0
	Receding angle	50.1±1.8	49.8±2.2	34.6±2.1
60-8-32	Advancing angle	64.9±2.1	64.8±1.9	46.3±1.8
	Receding angle	52.1±2.2	52.4±1.8	37.9±1.7

contents of 60 and 80 wt%. For the PMMA-*co*-PMAAM copolymer, the amide nitrogen atom's N 1 s peak is located at 403.7 eV. The intensity of the N 1 s peaks of the poly(MMA-*co*-MAAM-*co*-S) terpolymers decreased upon increasing the PS content; each peak can be deconvoluted into two peaks at 404.6 and 402.4 eV because the PS and PMAAM units of the copolymer do not experience any specific interactions [20–21]. The presence of N 1 s peaks is evidenced in the spectra of all the poly(MMA-*co*-MAAM-*co*-S) terpolymers, which indicates that the nitrogen atoms in PMAAM interact with PMAAM and PMMA units through self- and inter-associative hydrogen bonding, respectively. A decrease of ca. 2.0 eV in the value of the binding energy of N 1 s indicates that the PS monomer plays a role strictly as an inert diluent segment of the PMAAM polymer chain that reduces the degree of hydrogen bonding. The results are obvious when the PMMA content is 60 wt% because the intermolecular hydrogen bonding of PMAAM results in its being unable to interact with PMMA completely. In addition, the styrene plays the role of an inert diluent segment on the PMMA main chain, which results in an enhancement of the specific interactions between the amide groups of PMAAM and the functional groups of the second polymer by reducing the strong self-association of the PMAAM units.

Fig. 6 displays the O 1 s core-level spectra of poly(MMA-*co*-MAAM-*co*-S) terpolymers containing PMMA contents of 60 and 80 wt%. The binding energy of the O 1 s electrons of poly(MMA-*co*-MAAM-*co*-S) terpolymers decreases upon the addition of PS units. The value of the binding energy of the O 1 s electrons of the PMMA-*co*-PMAAM copolymer is higher than the corresponding binding energy of the poly(MMA-*co*-MAAM-*co*-S) terpolymers because of the weak self-associative hydrogen

Table 5
Surface energies of poly(MMA-*co*-MAAM-*co*-S) thin film terpolymers using the three-liquid LWAB method

Compositions PMMA-PMAAM-PS	γ^{LW}	γ^-	γ^+	γ^{AB}	γ
90-10-0	39.90	15.67	0.00	0.00	39.90
90-8-2	39.67	14.53	0.00	0.00	39.67
90-6-4	39.21	14.53	0.00	0.00	39.21
90-4-6	39.09	13.85	0.00	0.00	39.09
90-2-8	38.76	14.07	0.00	0.00	38.76
85-15-0	41.06	16.05	0.01	0.80	41.86
85-12-3	39.65	15.09	0.00	0.39	40.04
85-9-6	39.54	15.63	0.00	0.16	39.70
85-6-9	38.69	14.24	0.00	0.00	38.69
85-3-12	38.55	14.36	0.00	0.00	38.55
80-20-0	42.20	18.29	0.04	1.71	43.91
80-16-4	41.45	17.93	0.02	1.10	42.55
80-12-8	39.09	18.59	0.01	0.86	39.95
80-8-12	38.76	16.95	0.00	0.33	39.09
80-4-16	38.12	15.83	0.00	0.00	38.12
60-40-0	45.34	20.90	0.41	5.88	51.22
60-32-8	42.76	19.99	0.33	5.15	47.91
60-24-16	40.64	19.51	0.19	3.87	44.51
60-16-24	38.13	20.91	0.08	2.64	40.77
60-8-32	36.29	20.02	0.05	1.91	38.20

bonding within the PMMA-*co*-PMAAM copolymer that results from the presence of PS moiety. Furthermore, the O 1 s peak shifts significantly to the low-binding-energy side as the PS content increase, which indicates that the electron density of the oxygen atoms increases as a result of the sharing of their electron clouds between intramolecular and intermolecular hydrogen bonds. Fig. 6b indicates that the O 1 s peaks of the poly(MMA-*co*-MAAM-*co*-S) terpolymers having PMMA content of 80 wt% can be deconvoluted into two component peaks: one remains at 534.6 eV and the other appears at ca. 532.2 eV [22]. In the case where the PMMA content is 60 wt%, however, the O 1 s peaks of the poly(MMA-*co*-MAAM-*co*-S) terpolymers have complicated distributions because of sharing of the electron clouds of the O atoms between PMMA and PMAAM [23]. In addition, the intensity of the O 1 s peak decreases upon increasing the PS content, which corresponds to the decrease in the density of these O atoms.

Table 6
Hysteresis calculated from advancing and receding contact angles for water, diiodomethane (DIM), and ethylene glycol (EG) on the poly(MMA-*co*-MAAM-*co*-S) thin film terpolymers

Compositions PMMA-PMAAM-PS	δ_w	δ_g	δ_d
90-10-0	0.49	0.39	0.44
90-8-2	0.44	0.32	0.36
90-6-4	0.23	0.35	0.34
90-4-6	0.22	0.29	0.26
90-2-8	0.28	0.18	0.22
85-15-0	0.97	0.79	0.84
85-12-3	0.67	0.62	0.79
85-9-6	0.59	0.46	0.65
85-6-9	0.36	0.39	0.26
85-3-12	0.22	0.26	0.25
80-20-0	1.08	1.03	0.95
80-16-4	0.95	0.89	0.76
80-12-8	0.54	0.80	0.49
80-8-12	0.48	0.68	0.32
80-4-16	0.28	0.35	0.20
60-40-0	1.78	1.14	1.28
60-32-8	1.47	1.07	1.11
60-24-16	1.00	1.04	0.77
60-16-24	0.19	0.44	0.67
60-8-32	0.17	0.21	0.38

3.4. Surface energy calculation

Table 4 summarizes all of the advancing and receding contact angles, as well as their standard deviations, for the poly(MMA-*co*-MAAM-*co*-S) copolymers as a function of their monomer ratios. Because the advancing contact angle can be measured more precisely than the receding angle, hereafter we discuss only the advancing contact angle [24]. Table 4 indicates that the advancing angles of water, glycerol, and diiodomethane decrease as the PS content increases in the poly(MMA-*co*-MAAM-*co*-S) system. Clear trends are found for diiodomethane in the poly(MMA-*co*-MAAM-*co*-S) system containing 60 wt% PMMA moieties. Because of their large water contact angles, poly(MMA-*co*-MAAM-*co*-S) copolymers possess nonpolar surfaces at PMMA contents of 85 and 90 wt%.

Table 5 summarizes results of analyses, using the three-liquid Lifshitz–van der Waals acid–base (LWAB) method, of the surface energies of the poly(MMA-*co*-MAAM-*co*-S) systems. The total surface energy decreases as the PS content increases for all monomer ratios in the poly(MMA-*co*-MAAM-*co*-S) system. The Lewis acid component (γ^+)

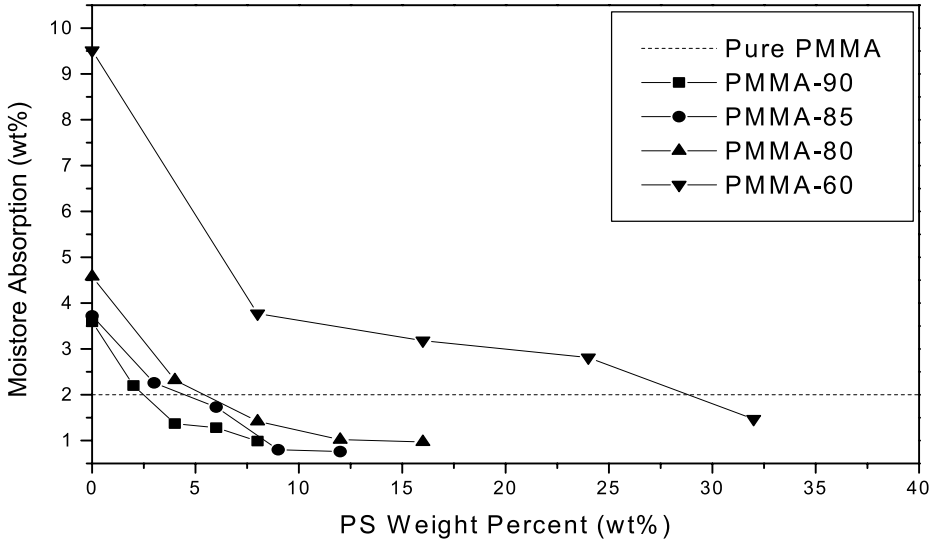

Fig. 7. Moisture absorption of poly(MMA-*co*-MAAM-*co*-S) terpolymers.

of the surface energy is close to zero for PMMA contents of 85 and 90 wt% in the poly(MMA-*co*-MAAM-*co*-S) system; this situation leads to a vanishing value of the donor–acceptor component (γ^{AB}) [25]. This result indicates that the PS monomer content in the PMAAM polymer chain containing 85 or 90 wt% PMMA does not change the polar component of the surface energy, but this polar component decreases upon increasing the PS content when the PMMA content in the poly(MMA-*co*-MAAM-*co*-S) system is either 60 or 80 wt%. This result implies that intramolecular hydrogen bonding in the poly(MMA-*co*-MAAM-*co*-S) system dictates the donor–acceptor component of the surface energy. In the case of a polar component in the surface energy, the value of γ^{LW} decreases upon the addition of PS moieties into the terpolymer system. We suggest two reasons for this effect: (1) the polarity of pure PS is lower than that of the PMMA-*co*-PMAAM and (2) the PS moiety reduces the strength of the intramolecular hydrogen bonding of the terpolymer and, thus, enhances the dispersed property in the surface energy through intermolecular hydrogen bonding.

We determined the hysteresis in the contact angle measurement from the quantity $\delta = |\cos(\theta_a)\text{-}\cos(\theta_r)|$, where θ_a and θ_r are the advancing and receding contact angles, respectively. Table 6 indicates that the average values of δ for all of the liquids we investigated on the surface of the poly(MMA-*co*-MAAM-*co*-S) terpolymer are dependent on the PS content. Phenomenological models [26–27] have suggested that hysteresis in the value of the contact angle is due to the presence of chemical or physical heterogeneities and/or slow surface reorganization (surface dynamics). On this basis, certain qualitative inferences can be made. The chemical or physical heterogeneity of the copolymer, which decreases upon the addition of PS units, is related to the dispersed property of the surface energy. A clear trend is found in the poly(MMA-*co*-MAAM-*co*-S) system containing 60 wt% PMMA. This observation suggests that intra-molecular hydrogen bonding induces aggregate of homogeneous polymer, resulting in chemical or physical heterogeneity on the terpolymer's surface, whereas the intermolecular hydrogen bonding diminishes the aggregate of homogeneous polymer, resulting in decrease of chemical or physical heterogeneity on the terpolymer surface.

3.5. Moisture absorption analyses

PMMA is highly moisture absorptive because its carbonyl groups form hydrogen bonds with water. Therefore, providing greater hydrophobic character is required to reduce the moisture absorptive property of our terpolymer system. PS possesses low water absorption ability because of its nonpolar structure and hydrophobic properties. Fig. 7 displays the moisture absorption of pure PMMA and several poly(MMA-*co*-MAAM-*co*-S) terpolymers. Compared with pure PMMA, the moisture absorption increases upon increasing the PMAAM content in the PMAAM-*co*-PMMA copolymers, but it is clear that the moisture absorption decreases upon increasing the PS content in PMMA terpolymers. It is interesting to note that certain selected copolymers exhibit lower moisture absorption, but higher values of T_g, than that exhibited by pure PMMA. These selected copolymers have the potential to replace pure PMMA in optical device applications.

4. Conclusions

We have found that positive deviations arise in the value of T_g as a function of composition, based on the Kwei equation, as a result of strong hydrogen bonding interactions existing in the main chains of PMAAM-*co*-PMMA

copolymers, but that such strong hydrogen bonding tends to increase moisture absorption. By incorporating styrene moieties into the PMAAM-*co*-PMMA main chain results in lower moisture absorption. In certain selected terpolymers, the moisture absorption is lower, but the value of T_g is higher, than that of pure PMMA. These selected copolymers have the potential to replace pure PMMA in optical device applications. We found that the intermolecule hydrogen bonding within terpolymers diminishes the aggregate of homogeneous polymer, resulting in the decrease of surface energy because of the chemical or physical homogeneity in terpolymer system. XPS analysis demonstrated that surface enrichment of the terpolymer occurred upon addition of PS. The results indicate that (1) the surface enrichment in hydrogen-bonding copolymers responds to changes in the surface energies of the PMAAM-*co*-PMMA main chain and (2) hydrogen bonding interactions reduce surface enrichment.

Acknowledgements

This research was financially supported by the National Science Council, Taiwan, Republic of China, under Contract Nos. NSC-93-2216-E-009-018.

References

[1] Yuichi K. J Appl Polym Sci 1997;63:363.
[2] Otsu T, Motsumoto T. Polym Bull 1990;23:43.
[3] Braun D, Czerwinski WK. Makromol Chem 1987;188:2389.
[4] Kuo SW, Kao HC, Chang FC. Polymer 2003;44:6873.
[5] Coleman MM, Xu Y, Painter PC. Macromolecules 1994;27:127.
[6] Kuo SW, Xu H, Huang CF, Chang FC. J Polym Sci, Polym Phys Ed 2002;40:2313.
[7] Kao HC, Kuo SW, Chang FC. J Polym Res 2003;10:111.
[8] Coleman MM, Graf JF, Painter PC. Specific interactions and the miscibility of polymer blends. Lancaster PA: Technomic Publishing; 1991.
[9] Kuo SW, Chang FC. Macromolecules 2001;34:5224.
[10] Kuo SW, Chang FC. Macromolecules 2001;34:7737.
[11] Goh SH, Lee SY, Zhou X, Tan KL. Macromolecules 1999;32:942.
[12] Goh SH, Lee SY, Zhou X, Tan KL. Macromolecules 1998;31:4260.
[13] Jiao H, Goh SH, Valiyaveettil S. Macromolecules 2001;34:7162.
[14] Van Oss CJ, Chaudhury MK, Good RJ. Chem Rev 1988;88:927.
[15] Van Oss CJ, Ju L, Chaudhury MK, Good RJ. J Colloid Interface Sci 1989;128:313.
[16] Fowkes FM. J Phys Chem 1962;66:382.
[17] Kaye GWC, Laby TH, editors. Table of physical and chemical constants. Harlow: Longman Scientific and Technical; 1992.
[18] Lide DR, editor. Handbook of chemistry and physics. 76th ed., CRC Press; 1995.
[19] Odian G. Principles of polymerization. New York: Wiley Publication; 1991, p. 470.
[20] Goh SH, Lee SY, Zhou X. Macromolecules 1998;31:4260.
[21] Yi J, Goh SH. Macromolecules 2001;34:4662.
[22] Liu S, Chan CM, Weng LT, Lin L, Jiang M. Macromolecules 2002; 35:5623.
[23] Liu S, Jiang M, Chan CM, Weng LT. Macromolecules 2001;34:3802.
[24] Ma KX, Chung T. J Phys Chem B 2001;105:4145.
[25] Tsibouklis J, Stone M, Thorpe AA, Graham P, Nevel TG, Ewen RJ. Langmuir 1999;15:7076.
[26] Good RJ. J Am Chem SOC 1952;74:5041.
[27] Morra M, Occhiello E, Garbassi F. Adv Colloid Interface Sci 1990;32: 79.